molecular pharmaceutics

Article

pubs.acs.org/molecularpharmaceutics

Improved Intraoperative Detection of Ovarian Cancer by Folate Receptor Alpha Targeted Dual-Modality Imaging

Marlène C. H. Hekman,*[,†,‡] Otto C. Boerman,[†] Desirée L. Bos,[†] Leon F. A. G. Massuger,[§] Susan Weil,[∥] Luigi Grasso,[∥] Katherine A. Rybinski,[∥] Egbert Oosterwijk,[‡] Peter F. A. Mulders,[‡] and Mark Rijpkema[†]

[†]Department of Radiology and Nuclear Medicine, Radboudumc, Nijmegen 6525 GA, Netherlands

[‡]Department of Urology, Radboudumc, Nijmegen 6525 GA, Netherlands

[§]Department of Gynecology, Radboudumc, Nijmegen 6525 GA, Netherlands

[∥]Morphotek, Exton, Pennsylvania 19341, United States

Supporting Information

ABSTRACT: Complete resection of tumor lesions in advanced stage ovarian cancer patients is of utmost importance, since the extent of residual disease after surgery strongly affects survival. Intraoperative imaging may be useful to improve surgery in these patients. Farletuzumab is a humanized IgG1 antibody that specifically recognizes the folate receptor alpha (FRα). Labeled with a radiolabel and a fluorescent dye, farletuzumab may be used for the intraoperative detection of ovarian cancer lesions. The current aim is to demonstrate the feasibility of FRα-targeted dual-modality imaging using ^{111}In-farletuzumab-IRDye800CW in an intraperitoneal ovarian cancer model. Biodistribution studies were performed 3 days after injection of 3, 10, 30, or 100 μg of ^{111}In-farletuzumab-IRDye800CW in mice with subcutaneous IGROV-1 tumors (5 mice per group). In mice with intraperitoneal IGROV-1 tumors the nonspecific uptake of ^{111}In-farletuzumab-IRDye800CW was determined by coinjecting an excess of unlabeled farletuzumab. MicroSPECT/CT and fluorescence imaging were performed 3 days after injection of 10 μg of ^{111}In-farletuzumab-IRDye800CW. FRα expression in tumors was determined immunohistochemically. Optimal tumor-to-blood-ratios (3.4−3.7) were obtained at protein doses up to 30 μg. Multiple intra-abdominal tumor lesions were clearly visualized by microSPECT/CT, while uptake in normal tissues was limited. Fluorescence imaging was used to visualize and guide resection of superficial tumors. Coinjection of an excess of unlabeled farletuzumab significantly decreased tumor uptake of ^{111}In-farletuzumab-IRDye800CW (69.4 ± 27.6 versus 18.3 ± 2.2% ID/g, $p < 0.05$). Immunohistochemical analyses demonstrated that the radioactive and fluorescent signal corresponded with FRα-expressing tumor lesions. FRα-targeted SPECT/fluorescence imaging using ^{111}In-farletuzumab-IRDye800CW can be used to detect ovarian cancer *in vivo* and could be a valuable tool for enhanced intraoperative tumor visualization in patients with intraperitoneal metastases of ovarian cancer.

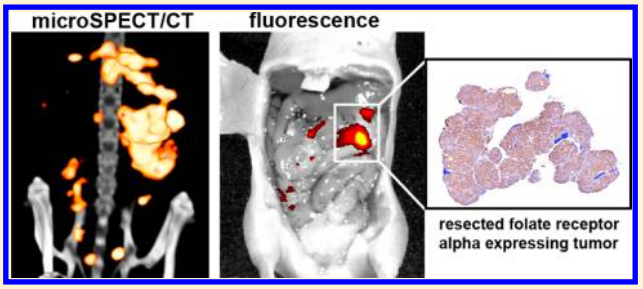

KEYWORDS: *ovarian cancer, molecular imaging, near-infrared fluorescence imaging, image-guided surgery, folate receptor alpha targeted imaging*

INTRODUCTION

Epithelial ovarian cancer is also called the "silent lady killer", since clinical symptoms arise relatively late.[1] As a consequence, approximately 70% of patients present with disease extending to other structures within or outside the pelvis at time of diagnosis.[1] Ovarian cancer metastasizes primarily throughout the abdominal cavity, and complete resection of tumor lesions is of utmost importance.[2] These patients can be treated by primary debulking surgery or by neoadjuvant chemotherapy followed by surgery (interval debulking).[2] In both regimes, the extent of residual disease after surgery is one of the main prognostic factors for (progression free) survival.[1−4] Especially in patients previously treated with chemotherapy the distinction between tumor tissue and benign tissue can be challenging during surgery, since tumor lesions may shrink or visually disappear due to chemotherapy.[2] Intraoperative tumor-specific imaging may be useful to improve surgery of ovarian cancer patients as it may facilitate accurate and sensitive detection of tumor tissue.

Van Dam et al. have shown that FRα-targeted fluorescence imaging using folate-FITC (EC17) can be beneficial in staging and debulking of metastatic ovarian cancer patients.[5] The FRα is overexpressed in approximately 90% of the ovarian carcinomas, while expression in normal tissue is limited.[6,7] Furthermore, the expression of the FRα is not changed by chemotherapy.[8] Therefore, the receptor has been proposed as an ideal marker for targeted therapies and targeted imaging in

Received: June 7, 2017
Revised: July 25, 2017
Accepted: August 21, 2017
Published: August 21, 2017

DOI: 10.1021/acs.molpharmaceut.7b00464
Mol. Pharmaceutics 2017, 14, 3457−3463

ovarian cancer patients.[9,10] Farletuzumab (also designated as MORAb-003) is an intact humanized IgG1 antibody that specifically recognizes FRα and is investigated as a diagnostic as well as a therapeutic agent for ovarian cancer.[11−13] Phase I/II therapeutic clinical trials have shown no dose-limiting toxicities, and a pilot clinical study has shown that single photon emission computed tomography (SPECT) after injection of ^{111}In-farletuzumab can detect ovarian cancer and metastases.[11,12,14,15]

Fluorescently labeled farletuzumab may enable intraoperative imaging, but the limited penetration depth of light in biological tissues implies that only superficial tumor lesions can be detected. Therefore, the use of dual-labeled tracers might be advantageous: the radioactive signal can be used to detect deeply located tumors, while the fluorescent label allows for accurate real-time tumor delineation. Several preclinical studies have shown the feasibility of targeted dual-modality imaging using monoclonal antibodies.[16−22]

The aim of the current study is to show the feasibility of FRα-targeted dual-modality imaging in ovarian cancer using ^{111}In-farletuzumab-IRDye800CW in an intraperitoneal tumor model.

MATERIALS AND METHODS

Animals. Animal studies were performed after approval of the national committee on animal experiments (CCD) and the local animal welfare body (AWB). BALB/c nu/nu mice (6−8 weeks old) were obtained from Janvier (Le Genest-Saint-Isle, France) and acclimatized to laboratory conditions during 1 week. Mice were fed water and animal chow ad libitum. At least 48 h before the start of the image-guided surgery and biodistribution experiments, mice were fed a folate-free diet. Daily health monitoring was performed. Mice with ip tumors were weighed three times a week as part of their welfare assessment.

Dual-Labeled Antibody Production. Dual-labeled farletuzumab was produced essentially as previously described.[17] In short, 2.5 mg of humanized farletuzumab (5 mg/mL, IgG1, Morphotek, Exton, PA) was incubated at room temperature during 1 h with 58 μg of IRDye800CW-NHS ester (LI-COR biosciences, Lincoln, NE) in 0.1 M $NaHCO_3$, pH 8.5. Next, farletuzumab-IRDye800CW was incubated with 109 μg of ITC-DTPA (Macrocyclics, Dallas, TX) in 0.1 M $NaHCO_3$, pH 9.5. Unconjugated IRDye800CW and ITC-DTPA were removed by extensive dialysis against 0.25 M ammonium acetate, pH 5.5. On average 1.7 molecules of IRDye800CW were conjugated per antibody (substitution ratio) as was determined with the Ultrospec 2000 UV/visible spectrophotometer (Pharmacia Biotech, Sweden). The absorption and emission spectra of DTPA-farletuzumab-IRDye800CW and IRDye800CW were measured with a microplate reader (Infinite Pro 200, Tecan Austria GmbH, Groedig, Austria) (Figure S1). The immunoreactive fraction of dual-labeled farletuzumab was determined after 1 h incubation with IGROV-1 cells as described by Lindmo et al.[23] and exceeded 70%. DTPA-farletuzumab-IRDye800CW was stored in the dark at 4 °C until radiolabeling.

$^{111}InCl_3$ was purchased from Mallinckrodt Pharmaceuticals ('s Hertogenbosch, The Netherlands). On the day of the experiments radiolabeling of DTPA-farletuzumab-IRDye800CW with indium-111 was performed by 30 min incubation at room temperature in 0.5 M MES buffer, pH 5.0. Radiochemical purity was determined by instant thin layer chromatography (ITLC) on silica gel strips, using 0.1 M sodium citrate buffer, pH 6.0 as mobile phase and always exceeded 95%. To reach a specific activity of 1.25 MBq/μg for SPECT imaging, dual-labeled farletuzumab was purified after radiolabeling using a PD10 column with 0.5% BSA/PBS. After purification (ITLC > 95%), 79% of the original amount of protein was left, and this was supplemented with unlabeled DTPA-farletuzumab-IRDye800CW to the desired protein dose. For the dose escalation studies an equivalent of 3 μg of DTPA-farletuzumab-IRDye800CW per mouse was labeled with indium-111 and subsequently supplemented to the desired protein dose with unlabeled DTPA-farletuzumab-IRDye800CW. Before iv injection, the injection volume was adjusted to 200 μL per mouse with 0.5% BSA/PBS.

Dose Escalation Study (Sc Tumor Model). To determine the optimal protein dose to perform dual-modality imaging, a protein dose escalation study was performed in mice with sc IGROV-1 xenografts. Cells were cultured in RPMI medium enriched with 10% fetal calf serum and 1% glutamine. Mice were injected sc with 200 μL of tumor cell suspension (10^7 cells) on the right flank. When tumors had grown to approximately 100 to 300 mm^3, mice were injected iv with 10 μg of ^{111}In-farletuzumab-IRDye800CW (0.5 MBq). After approximately 1.5 weeks of tumor growth, mice were injected iv with 3, 10, 30, or 100 μg of ^{111}In-farletuzumab-IRDye800CW (5 per group, 0.5 MBq/mouse, 200 μL/mouse). Three days after injection, fluorescence imaging was performed with the IVIS Lumina closed-cabinet fluorescence scanner (excitation 745 nm, background correction excitation 640 nm, emission filter ICG, field of view *C*, binning medium, *f*-stop 2). Additionally, biodistribution studies were performed (see below).

Dual-Modality Imaging and Image-Guided Surgery (Ip Tumor Model). To show the feasibility of fluorescence imaging and fluorescence-guided surgery in a setting relevant for ovarian cancer, an ip tumor model with IGROV-1 cells was optimized. As a pilot study to assess tumor growth 12 mice were injected ip with 10^6 or 5×10^6 IGROV-1 cells in 500 μL of RPMI (6 mice per group). Mice were injected iv with dual-labeled farletuzumab after 3, 7, or 13 days of tumor growth (2 mice per time point per group). Three days later fluorescence imaging and biodistribution studies were performed (days 6, 10, and 16 respectively).

Next, the feasibility of dual-modality imaging and fluorescence-guided surgery was studied in 8 mice with ip tumors. Seven days after tumor inoculation (5×10^6 cells), mice received 10 μg of dual-labeled farletuzumab (12.5 MBq/mouse, iv). To determine the nonspecific tumor uptake of dual-labeled farletuzumab, 3 out of the 8 mice were coinjected with an excess of unlabeled farletuzumab (1 mg) to block the FRα *in vivo*. After 10 days of tumor growth (3 days p.i.) dual-modality imaging and fluorescence-guided surgery were performed. Mice were euthanized by O_2/CO_2 suffocation. Then, SPECT/CT imaging was performed in the USPECT small animal scanner (Milabs, Utrecht, The Netherlands) using a 1.0 mm mouse pinhole collimator (2 × 15 min acquisition time, 28 bed positions). SPECT/CT images were reconstructed using the MILabs software (Utrecht, The Netherlands; reconstruction parameters 0.2 mm voxels, 16 subsets, 4 iterations, Gaussian filter 1.5) and subsequently analyzed using the Inveon Research Workplace (Siemens Healthcare, The Netherlands). Next, fluorescence images were obtained with the IVIS Lumina closed-cabinet fluorescence scanner (Caliper LifeSciences, Hopkinton, MA) after removal of the abdominal skin

DOI: 10.1021/acs.molpharmaceut.7b00464
Mol. Pharmaceutics 2017, 14, 3457−3463

(excitation 745 nm, background correction excitation 640 nm, emission filter ICG, field of view B, binning small, *f*-stop 2). After resection of all visible tumor lesions, mice were imaged again with the IVIS Lumina to check for residual disease. Finally, biodistribution studies were performed (see below).

Five micrometer sections were cut from formalin-fixed and paraffin-embedded resected tumor tissue and analyzed autoradiographically. Sections were exposed for 2 weeks to a phosphor imaging plate and developed using the Typhoon FLA 7000 phosphor imager (GE Healthcare Life Sciences, Eindhoven, The Netherlands). Then, the fluorescent signal in the tumor sections was imaged with the Odyssey CLx flatbed fluorescence scanner (800 nm channel, recording time 1−5 min, focus 1.0 mm) (LI-COR biosciences, Lincoln, NE). Lastly, a standard hematoxylin and eosin staining was performed, as well as a folate-receptor-alpha-staining using the Folate Receptor alpha IHC Assay Kit (Morphotek, Exton, PA).

Biodistribution Studies. All studies were performed 3 days after injection of dual-labeled farletuzumab. For biodistribution studies samples of blood, muscle, heart, lung, spleen, kidney, pancreas, liver, stomach, duodenum, and tumor lesions were retrieved. Tissue samples were weighed and measured in a gamma counter (2480 WIZARD,[2] PerkinElmer, Boston, MA) together with standards of the injected dose in triplicate. The accumulation of dual-labeled farletuzumab was expressed as percentage of the injected dose per gram of tissue (% ID/g), and values are represented as mean ± standard deviation (SD).

Statistical analyses were performed using IBM SPSS Statistics 22.0. In the dose escalation study a one-way ANOVA test with post hoc Bonferroni correction was performed to test for significant differences in tumor accumulation between the different dose levels. Tumor uptake in the mice that received an excess of unlabeled farletuzumab was tested for significance with an independent sample *t* test. An alpha of 0.05 was used in all analyses; $p < 0.05$ was considered significant.

RESULTS

Dose Escalation Study (Sc Tumor Model). The protein dose-escalation study revealed tumor-to-blood-ratios of 3.5, 3.4, 3.7, and 2.8 in the 3, 10, 30, and 100 μg dose levels, respectively. Tumor uptake was 43.6 ± 4.8, 39.9 ± 4.3, 39.3 ± 5.8, and 32.7 ± 3.2% ID/g after injection of 3, 10, 30, and 100 μg dual-labeled farletuzumab respectively (Figure 1). Tumor uptake after injection of 100 μg of dual-labeled farletuzumab was significantly lower than tumor uptake after injection of 3 μg ($p < 0.05$). No significant differences in tumor uptake between the 3, 10, and 30 μg dose levels were seen. Further studies were performed with a protein dose of 10 μg of dual-labeled farletuzumab.

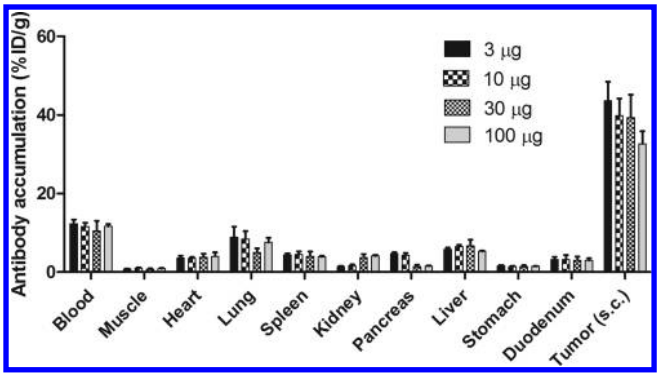

Figure 1. Biodistribution profiles of indium-111-farletuzumab-IRDye800CW 3 days p.i. in BALB/c nu/nu mice with sc IGROV-1 tumors at four different protein doses.

Dual-Modality Imaging and Fluorescence-Guided Surgery (Ip Tumor Model). Fluorescence imaging clearly visualized high uptake of dual-labeled farletuzumab in macroscopically visible tumor lesions as early as 6 days after tumor cell injection in 10 out of 12 mice. Tumors were mainly located around the spleen, in the hepatic hilum and between the abdominal organs. Two mice that were injected with 10^6 IGROV-1 cells did not have visible ip tumors, and in one mouse no tumors could be visualized with fluorescence imaging (only biodistribution studies were performed in the second mouse). No tumor lesions outside the abdominal cavity were observed during extensive macroscopic inspection, and mice did not develop ascites.

Uptake of ^{111}In-farletuzumab-IRDye800CW was visualized by microSPECT/CT in multiple intra-abdominal lesions in all 5 mice that were injected with 10 μg/12.5 MBq ^{111}In-farletuzumab-IRDye800CW (Figures 2a and 2b). After resection of the abdominal skin, the gross majority of these hotspots could be localized to macroscopic tumor deposits and were detectable with fluorescence imaging (Figures 2c and 2d). For superficial tumors microSPECT images matched with the corresponding fluorescence images (Figure 2). Intraoperative fluorescence imaging was used to guide resection of superficial tumor lesions (Figure 3). After shifting the organs, also deeply seated tumor lesions could be visualized with fluorescence imaging (Figure S1a). However, it is more difficult to trace back the location of deeply located tumors in the abdomen to their preoperative location on the microSPECT/CT. In addition, fluorescence imaging revealed multiple lesions throughout the abdomen, suggestive of submillimeter tumor deposits that are barely visible to the naked eye (Figures 2d, 4, and S2).

Microscopic tissue studies demonstrated that the radioactive and fluorescent signal corresponded with FRα-expressing tumor lesions (Figures 4 and S3). The FRα-staining showed a very homogeneous FRα expression in the IGROV-1 tumors, but autoradiography and fluorescence imaging showed that the distribution of dual-labeled farletuzumab in tumor tissue was more heterogeneous (Figure S3). This difference may be due to differences in tumor vascularization. Coinjection of an excess of unlabeled farletuzumab resulted in a significant decrease of dual-labeled farletuzumab in tumor tissue (69.4 ± 27.6 versus 18.3 ± 2.2% ID/g, $p < 0.05$) (Figure S4), indicating that the accumulation of the dual-labeled antibody in the tumor was FRα-mediated.

DISCUSSION

This study shows the feasibility of FRα-targeted dual-modality image-guided surgery of ovarian cancer lesions using ^{111}In-farletuzumab-IRDye800CW. Intraperitoneal IGROV-1 tumor lesions were clearly visualized with both microSPECT/CT and fluorescence imaging, and dual-modality imaging was used to guide complete tumor resection. These results support the clinical translation of dual-modality imaging using dual-labeled farletuzumab, where it could be a valuable tool to assist the surgeon in cytoreductive surgery in patients with FRα-expressing tumors.

In the current study dual-modality imaging was optimized in mice with subcutaneous IGROV-1 xenografts. Biodistribution studies showed that optimal tumor-to-blood-ratios (3.4−3.7)

DOI: 10.1021/acs.molpharmaceut.7b00464
Mol. Pharmaceutics 2017, 14, 3457−3463

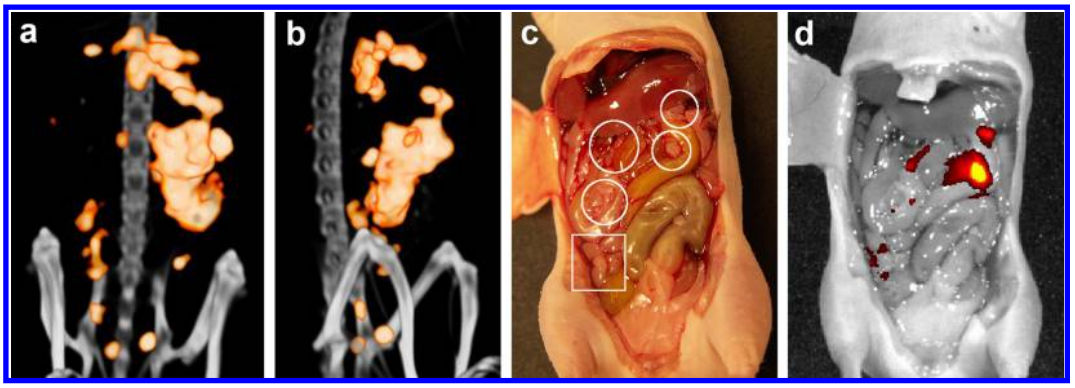

Figure 2. MicroSPECT/CT shows multiple intraperitoneal IGROV-1 tumors as small as 1 mm (a, coronal view; b, sagittal view). Due to the high tumor-to-normal tissue ratio and tumor-to-liver ratio, only uptake in tumor tissue is visualized. After resection of the abdominal skin, multiple tumor deposits were observed macroscopically (white circles in c) and were visualized with fluorescence imaging (d). Furthermore, fluorescence imaging identified additional tumor lesions that were barely visible with the naked eye (square in c).

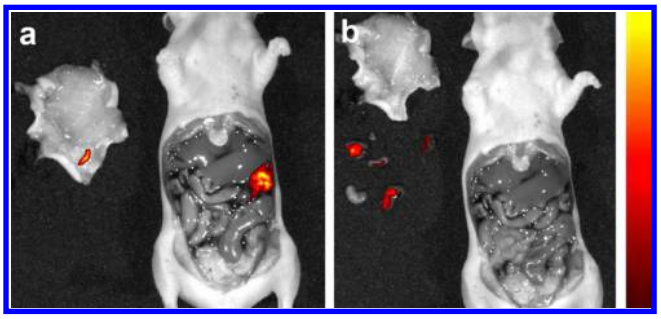

Figure 3. Detection of superficially located tumor lesions by fluorescence imaging (a) and fluorescence image-guided surgery of intraperitoneal IGROV-1 tumors (b).

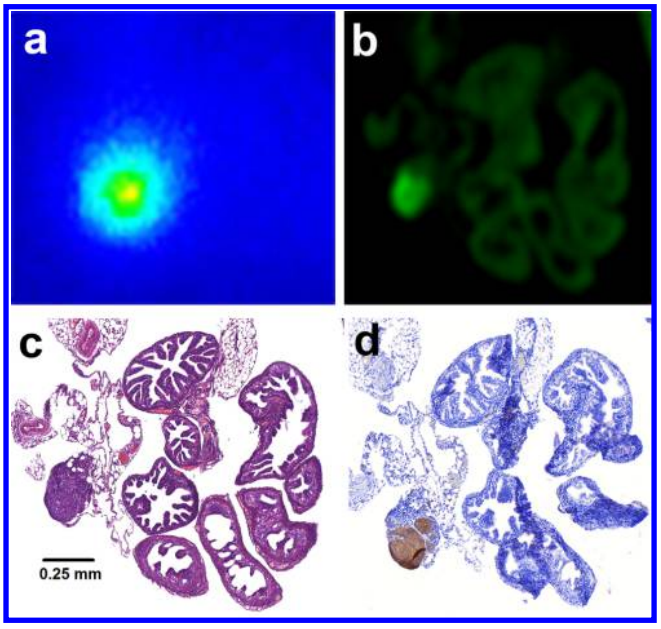

Figure 4. Autoradiography (a) and fluorescence imaging (b) of a tissue section of the mouse oviduct revealed an area with high accumulation of dual-labeled farletuzumab. H&E staining (c) of this same tissue section showed that this area corresponded with a 0.25 mm tumor lesion located near the oviduct. The FRα-staining on an adjacent tissue section confirmed that this lesion expressed FRα (d).

were achieved at protein doses up to 30 μg. The decreased tumor accumulation at higher protein doses probably relates to antigen saturation at higher protein doses as has been described previously.[24] The biodistribution and tumor accumulation (up to 43.6% ID/g in the sc model) of ^{111}In-farletuzumab-IRDye800CW were comparable to those of ^{111}In-DOTA-farletuzumab as previously reported by Smith-Jones et al. (tumor uptake 32% ID/g 4 days after injection).[14] This finding is in accordance with our previous studies that indicated that conjugation of an antibody with IRDye800CW up to a substitution ratio of 2 only marginally affects the *in vivo* behavior of the antibody.[17] Next, the feasibility of dual-modality imaging was shown in an ip tumor model. Preoperative microSPECT/CT identified FRα-expressing intra-abdominal tumor lesions as small as 1 mm (Figures 2a and 2b). Intraoperative fluorescence imaging successfully guided resection of superficially located tumor lesions (Figure 3). Microscopic analyses confirmed that the resected lesions were tumor lesions (Figure S3), and a colocalization was seen between the radioactive and fluorescent signal and FRα-expression (Figures 4 and S3). Coinjection of an excess of unlabeled farletuzumab resulted in significant reduction of accumulation of dual-labeled farletuzumab in tumor tissue (Figure S4). This indicates that the uptake of dual-labeled farletuzumab in tumor lesions is mainly due to specific binding of farletuzumab to FRα. However, nonspecific tracer uptake may also contribute to tumor accumulation because of the enhanced permeability and retention effect (EPR) in tumor lesions.

Since ovarian cancer mainly spreads within the abdominal cavity and lesions develop on the surface of abdominal organs, a clear contrast between tumors and the abdominal organs is a requirement for sensitive intraoperative detection of ovarian cancer lesions. In the current study, high accumulation of dual-labeled farletuzumab in tumor tissue was seen, while accumulation in the normal abdominal tissues was low as predicted by lack of farletuzumab's cross-reactivity to murine FRα. This led to a high tumor-to-normal contrast as shown in Figures 2 and 4. Thus, fluorescence imaging could be a useful aid to improve surgery of advanced stage ovarian cancer patients. In addition, fluorescence imaging could also be used to improve staging of ovarian cancer patients. Accurate staging of lower stage ovarian cancer patients is important to decide if adjuvant therapy is indicated. After comprehensive surgical staging approximately 30% of ovarian cancer patients are upstaged, since (micro)metastases are found in the uterus and/or fallopian tubes, in the lymph nodes, and in peritoneal,

DOI: 10.1021/acs.molpharmaceut.7b00464
Mol. Pharmaceutics 2017, 14, 3457−3463

omental, or adhesion biopsies.[25] Targeted intraoperative fluorescence imaging could guide the surgeon to tumor tissue and thereby improve staging and cytoreductive surgery.

A nontargeted fluorescence imaging approach based on the enhanced permeability and retention effect using indocyanine green has been investigated by Tummers et al.[26] In this study, ovarian cancer lesions appeared fluorescent, but a false-positive rate of 62% was found.[26] Currently, several trials are ongoing that demonstrate the value of targeted intraoperative fluorescence imaging.[5,27−29] The FRα is an ideal marker for targeted imaging in ovarian cancer patients, whereas the folate receptor beta has limited value, because it is expressed on activated macrophages and to a lesser extent on ovarian cancer lesions.[9,10,30] Recently it was shown that 16 to 29% additional lesions could be detected using FRα-targeted fluorescence imaging using folate-analogues (EC17 and OTL38).[31,32] A clear advantage of folate-analogues over using intact antibodies is the shorter time that is needed to obtain an optimal tumor-to-normal tissue contrast (several hours versus several days). However, false positive rates of 23% were found in both studies.[31,32] With EC17, this can partly be attributed to autofluorescence of benign tissue in the 500 nm range. Near-infrared fluorescence imaging with OTL38 has the advantage of lower autofluorescence and a higher tissue penetration depth, leading to a better tumor-to-normal tissue contrast, as shown previously.[33] Also, folate analogues are not FRα specific, but may also bind the folate receptor beta on activated macrophages.[31,32] ^{111}In-farletuzumab-IRDye800CW has the advantages that farletuzumab only recognizes FRα and that imaging can be performed in the near-infrared range.[34]

However, even in the near-infrared range, the penetration depth of light restricts fluorescence imaging to superficially located tumor lesions. The advantage of using a radiolabel is that it can be visualized preoperatively with SPECT/CT imaging and that it can be used intraoperatively to localize deeply seeded tumors with a gamma probe or hand-held SPECT camera. Using dual-labeled imaging, deeper tumors can first be localized with a gamma probe, and after surgical exposure fluorescence imaging can be used to guide tumor resection and assess the surgical cavity for residual disease. Due to the small size of a mouse, gamma probe detection was not feasible in this preclinical study. Dual-modality imaging may be achieved using a dual-labeled probe or coinjection of two separate agents. The disadvantage of coinjection of two separate agents is the potentially different biodistribution and clearance of the agents. In a dual-labeled approach the radiosignal and the fluorescent signal originate from the same molecule. This has the advantage that both signals can serve as an internal control for each other, e.g., a positive radiosignal in tissue precludes that the fluorescent signal is due to autofluorescence. Another advantage of using a radiolabel in the preclinical setting is that it allows for easy quantification of the accumulation of ^{111}In-farletuzumab-IRDye800CW in tissues, whereas the quantification of a fluorescent signal can be challenging.[35] When combining fluorescent dyes with radioisotopes, radiolysis of the fluorescent molecule may occur, a phenomenon that can be prevented by adding reactive oxygen scavengers like ascorbic acid.[36] Considering that radiolysis is limited with indium-111-labeled compounds that are injected shortly after radiolabeling,[36] no specific precautions were taken in the current study.

When translating the current results to the clinical situation, one has to consider that the sensitivity of the imaging systems used in the clinical situation differs from that of the ones used in preclinical studies. Furthermore, in the clinical setting tumors may be more heterogeneous in terms of FRα expression and tumor physiology compared to the tumors in this mouse model. These factors may lead to more variation in the tumor uptake of the tracer. The feasibility of FRα-targeted dual-modality imaging was shown in an ip IGROV-1 tumor model, but feasibility should be shown in additional FRα-expressing tumor models. Also, the tumor-targeting characteristics of our tracer could be further assessed by using bioluminescence imaging in a luciferase expressing IGROV-1 tumor model. Other limitations in the current study included the lack of farletuzumab's cross-reactivity to murine FRα which may be present in normal tissue, as well as that dual-modality imaging was performed in a nonascitic tumor model. Patients with advanced stage ovarian cancer often develop ascites in which circulating tumor cells will be present. This may lead to an increased background signal in preoperative SPECT images due to accumulation of dual-labeled farletuzumab in the ascites. However, this did not appear to be a problem in the previous studies where FRα-targeted imaging has been performed.[5,14] Since ascites is removed at the start of surgery, this phenomenon will not hamper intraoperative fluorescence imaging.

CONCLUSION

In conclusion, this study shows the feasibility of FRα-targeted SPECT/fluorescence imaging using ^{111}In-farletuzumab-IRDye800CW in ovarian cancer *in vivo*. The next step will be to evaluate the value of dual-modality imaging and fluorescence-guided surgery of advanced stage ovarian cancer patients.

ASSOCIATED CONTENT

Supporting Information

The Supporting Information is available free of charge on the ACS Publications website at DOI: 10.1021/acs.molpharmaceut.7b00464.

Absorption and emission spectra, fluorescence imaging, tissue section analysis of tumor, and specific uptake demonstration (PDF)

AUTHOR INFORMATION

Corresponding Author

*Department of Radiology & Nuclear Medicine, Radboud University Medical Center, Geert Grooteplein-Zuid 10, 6525 GA, Nijmegen. E-mail: marlene.hekman@radboudumc.nl. Tel: +31-24-3614048. Fax: +31-24-3618942.

ORCID

Marlène C. H. Hekman: 0000-0003-3736-3924

Notes

The authors declare the following competing financial interest(s): Susan Weil is the director of clinical development of Morphotek and Luigi Grasso is the Chief Scientific Officer of Morphotek.

REFERENCES

(1) Ledermann, J. A.; Raja, F. A.; Fotopoulou, C.; Gonzalez-Martin, A.; Colombo, N.; Sessa, C. Newly diagnosed and relapsed epithelial ovarian carcinoma: ESMO Clinical Practice Guidelines for diagnosis, treatment and follow-up. *Ann. Oncol.* **2013**, *24* (Suppl. 6), vi24−32.

DOI: 10.1021/acs.molpharmaceut.7b00464
Mol. Pharmaceutics 2017, 14, 3457−3463

(2) Vergote, I.; Trope, C. G.; Amant, F.; Kristensen, G. B.; Ehlen, T.; Johnson, N.; Verheijen, R. H.; van der Burg, M. E.; Lacave, A. J.; Panici, P. B.; Kenter, G. G.; Casado, A.; Mendiola, C.; Coens, C.; Verleye, L.; Stuart, G. C.; Pecorelli, S.; Reed, N. S. Neoadjuvant chemotherapy or primary surgery in stage IIIC or IV ovarian cancer. *N. Engl. J. Med.* **2010**, *363* (10), 943−53.
(3) Elattar, A.; Bryant, A.; Winter-Roach, B. A.; Hatem, M.; Naik, R. Optimal primary surgical treatment for advanced epithelial ovarian cancer. *Cochrane database of systematic reviews* **2011**, No. 8, CD007565.
(4) Aletti, G. D.; Gallenberg, M. M.; Cliby, W. A.; Jatoi, A.; Hartmann, L. C. Current management strategies for ovarian cancer. *Mayo Clin. Proc.* **2007**, *82* (6), 751−70.
(5) van Dam, G. M.; Themelis, G.; Crane, L. M.; Harlaar, N. J.; Pleijhuis, R. G.; Kelder, W.; Sarantopoulos, A.; de Jong, J. S.; Arts, H. J.; van der Zee, A. G.; Bart, J.; Low, P. S.; Ntziachristos, V. Intraoperative tumor-specific fluorescence imaging in ovarian cancer by folate receptor-alpha targeting: first in-human results. *Nat. Med.* **2011**, *17* (10), 1315−9.
(6) Kalli, K. R.; Oberg, A. L.; Keeney, G. L.; Christianson, T. J.; Low, P. S.; Knutson, K. L.; Hartmann, L. C. Folate receptor alpha as a tumor target in epithelial ovarian cancer. *Gynecol. Oncol.* **2008**, *108* (3), 619−26.
(7) Markert, S.; Lassmann, S.; Gabriel, B.; Klar, M.; Werner, M.; Gitsch, G.; Kratz, F.; Hasenburg, A. Alpha-folate receptor expression in epithelial ovarian carcinoma and non-neoplastic ovarian tissue. *Anticancer Res.* **2008**, *28* (6A), 3567−72.
(8) Crane, L. M.; Arts, H. J.; van Oosten, M.; Low, P. S.; van der Zee, A. G.; van Dam, G. M.; Bart, J. The effect of chemotherapy on expression of folate receptor-alpha in ovarian cancer. *Cell. Oncol.* **2012**, *35* (1), 9−18.
(9) Vergote, I. B.; Marth, C.; Coleman, R. L. Role of the folate receptor in ovarian cancer treatment: evidence, mechanism, and clinical implications. *Cancer Metastasis Rev.* **2015**, *34* (1), 41−52.
(10) Maurer, A. H.; Elsinga, P.; Fanti, S.; Nguyen, B.; Oyen, W. J.; Weber, W. A. Imaging the folate receptor on cancer cells with 99mTc-etarfolatide: properties, clinical use, and future potential of folate receptor imaging. *J. Nucl. Med.* **2014**, *55* (5), 701−4.
(11) Konner, J. A.; Bell-McGuinn, K. M.; Sabbatini, P.; Hensley, M. L.; Tew, W. P.; Pandit-Taskar, N.; Vander Els, N.; Phillips, M. D.; Schweizer, C.; Weil, S. C.; Larson, S. M.; Old, L. J. Farletuzumab, a humanized monoclonal antibody against folate receptor alpha, in epithelial ovarian cancer: a phase I study. *Clin. Cancer Res.* **2010**, *16* (21), 5288−95.
(12) Sasaki, Y.; Miwa, K.; Yamashita, K.; Sunakawa, Y.; Shimada, K.; Ishida, H.; Hasegawa, K.; Fujiwara, K.; Kodaira, M.; Fujiwara, Y.; Namiki, M.; Matsuda, M.; Takeuchi, Y.; Katsumata, N. A phase I study of farletuzumab, a humanized anti-folate receptor alpha monoclonal antibody, in patients with solid tumors. *Invest. New Drugs* **2015**, *33* (2), 332−40.
(13) Vergote, I.; Armstrong, D.; Scambia, G.; Teneriello, M.; Sehouli, J.; Schweizer, C.; Weil, S. C.; Bamias, A.; Fujiwara, K.; Ochiai, K.; Poole, C.; Gorbunova, V.; Wang, W.; O'Shannessy, D.; Herzog, T. J. A Randomized, Double-Blind, Placebo-Controlled, Phase III Study to Assess Efficacy and Safety of Weekly Farletuzumab in Combination With Carboplatin and Taxane in Patients With Ovarian Cancer in First Platinum-Sensitive Relapse. *J. Clin. Oncol.* **2016**, *34* (19), 2271−8.
(14) Smith-Jones, P. M.; Pandit-Taskar, N.; Cao, W.; O'Donoghue, J.; Philips, M. D.; Carrasquillo, J.; Konner, J. A.; Old, L. J.; Larson, S. M. Preclinical radioimmunotargeting of folate receptor alpha using the monoclonal antibody conjugate DOTA-MORAb-003. *Nucl. Med. Biol.* **2008**, *35* (3), 343−51.
(15) Kim, K. H.; Jelovac, D.; Armstrong, D. K.; Schwartz, B.; Weil, S. C.; Schweizer, C.; Alvarez, R. D. Phase 1b safety study of farletuzumab, carboplatin and pegylated liposomal doxorubicin in patients with platinum-sensitive epithelial ovarian cancer. *Gynecol. Oncol.* **2016**, *140* (2), 210−4.
(16) Lutje, S.; Rijpkema, M.; Franssen, G. M.; Fracasso, G.; Helfrich, W.; Eek, A.; Oyen, W. J.; Colombatti, M.; Boerman, O. C. Dual-modality image-guided surgery of prostate cancer with a radiolabeled fluorescent anti-PSMA monoclonal antibody. *J. Nucl. Med.* **2014**, *55* (6), 995−1001.
(17) Rijpkema, M.; Bos, D. L.; Cornelissen, A. S.; Franssen, G. M.; Goldenberg, D. M.; Oyen, W. J.; Boerman, O. C. Optimization of dual-labeled antibodies for targeted intraoperative imaging of tumors. *Molecular imaging* **2015**, *14*, 15−25.
(18) Rijpkema, M.; Oyen, W. J.; Bos, D.; Franssen, G. M.; Goldenberg, D. M.; Boerman, O. C. SPECT- and fluorescence image-guided surgery using a dual-labeled carcinoembryonic antigen-targeting antibody. *J. Nucl. Med.* **2014**, *55* (9), 1519−24.
(19) Hekman, M. C.; Boerman, O. C.; de Weijert, M.; Bos, D. L.; Oosterwijk, E.; Langenhuijsen, J. F.; Mulders, P. F.; Rijpkema, M. Targeted Dual-Modality Imaging in Renal Cell Carcinoma: An Ex Vivo Kidney Perfusion Study. *Clin. Cancer Res.* **2016**, *22* (18), 4634−42.
(20) Hernandez, R.; Sun, H.; England, C. G.; Valdovinos, H. F.; Ehlerding, E. B.; Barnhart, T. E.; Yang, Y.; Cai, W. CD146-targeted immunoPET and NIRF Imaging of Hepatocellular Carcinoma with a Dual-Labeled Monoclonal Antibody. *Theranostics* **2016**, *6* (11), 1918−33.
(21) Zhang, Y.; Hong, H.; Severin, G. W.; Engle, J. W.; Yang, Y.; Goel, S.; Nathanson, A. J.; Liu, G.; Nickles, R. J.; Leigh, B. R.; Barnhart, T. E.; Cai, W. ImmunoPET and near-infrared fluorescence imaging of CD105 expression using a monoclonal antibody dual-labeled with (89)Zr and IRDye 800CW. *Am. J. Transl. Res.* **2012**, *4* (3), 333−46.
(22) Hong, H.; Zhang, Y.; Severin, G. W.; Yang, Y.; Engle, J. W.; Niu, G.; Nickles, R. J.; Chen, X.; Leigh, B. R.; Barnhart, T. E.; Cai, W. Multimodality imaging of breast cancer experimental lung metastasis with bioluminescence and a monoclonal antibody dual-labeled with 89Zr and IRDye 800CW. *Mol. Pharmaceutics* **2012**, *9* (8), 2339−49.
(23) Lindmo, T.; Boven, E.; Cuttitta, F.; Fedorko, J.; Bunn, P. A., Jr. Determination of the immunoreactive fraction of radiolabeled monoclonal antibodies by linear extrapolation to binding at infinite antigen excess. *J. Immunol. Methods* **1984**, *72* (1), 77−89.
(24) Steffens, M. G.; Oosterwijk-Wakka, J. C.; Zegwaart-Hagemeier, N. E.; Boerman, O. C.; Debruyne, F. M.; Corstens, F. H.; Oosterwijk, E. Immunohistochemical analysis of tumor antigen saturation following injection of monoclonal antibody G250. *Anticancer Res.* **1999**, *19* (2A), 1197−200.
(25) Garcia-Soto, A. E.; Boren, T.; Wingo, S. N.; Heffernen, T.; Miller, D. S. Is comprehensive surgical staging needed for thorough evaluation of early-stage ovarian carcinoma? *Am. J. Obstet. Gynecol.* **2012**, *206* (3), 242.e1−5.
(26) Tummers, Q. R.; Hoogstins, C. E.; Peters, A. A.; de Kroon, C. D.; Trimbos, J. B.; van de Velde, C. J.; Frangioni, J. V.; Vahrmeijer, A. L.; Gaarenstroom, K. N. The Value of Intraoperative Near-Infrared Fluorescence Imaging Based on Enhanced Permeability and Retention of Indocyanine Green: Feasibility and False-Positives in Ovarian Cancer. *PLoS One* **2015**, *10* (6), e0129766.
(27) de Boer, E.; Warram, J. M.; Tucker, M. D.; Hartman, Y. E.; Moore, L. S.; de Jong, J. S.; Chung, T. K.; Korb, M. L.; Zinn, K. R.; van Dam, G. M.; Rosenthal, E. L.; Brandwein-Gensler, M. S. In Vivo Fluorescence Immunohistochemistry: Localization of Fluorescently Labeled Cetuximab in Squamous Cell Carcinomas. *Sci. Rep.* **2015**, *5*, 10169.
(28) Rosenthal, E. L.; Warram, J. M.; de Boer, E.; Chung, T. K.; Korb, M. L.; Brandwein-Gensler, M.; Strong, T. V.; Schmalbach, C. E.; Morlandt, A. B.; Agarwal, G.; Hartman, Y. E.; Carroll, W. R.; Richman, J. S.; Clemons, L. K.; Nabell, L. M.; Zinn, K. R. Safety and Tumor Specificity of Cetuximab-IRDye800 for Surgical Navigation in Head and Neck Cancer. *Clin. Cancer Res.* **2015**, *21*, 3658.
(29) Keating, J. J.; Okusanya, O. T.; De Jesus, E.; Judy, R.; Jiang, J.; Deshpande, C.; Nie, S.; Low, P.; Singhal, S. Intraoperative Molecular Imaging of Lung Adenocarcinoma Can Identify Residual Tumor Cells at the Surgical Margins. *Molecular imaging and biology: MIB: the official publication of the Academy of Molecular Imaging* **2016**, *18* (2), 209−18.
(30) de Boer, E.; Crane, L. M.; van Oosten, M.; van der Vegt, B.; van der Sluis, T.; Kooijman, P.; Low, P. S.; van der Zee, A. G.; Arts, H. J.;

DOI: 10.1021/acs.molpharmaceut.7b00464
Mol. Pharmaceutics 2017, 14, 3457−3463

van Dam, G. M.; Bart, J. Folate Receptor-Beta Has Limited Value for Fluorescent Imaging in Ovarian, Breast and Colorectal Cancer. *PLoS One* **2015**, *10* (8), e0135012.
(31) Hoogstins, C. E.; Tummers, Q. R.; Gaarenstroom, K. N.; de Kroon, C. D.; Trimbos, J. B.; Bosse, T.; Smit, V. T.; Vuyk, J.; van de Velde, C. J.; Cohen, A. F.; Low, P. S.; Burggraaf, J.; Vahrmeijer, A. L. A Novel Tumor-Specific Agent for Intraoperative Near-Infrared Fluorescence Imaging: A Translational Study in Healthy Volunteers and Patients with Ovarian Cancer. *Clin. Cancer Res.* **2016**, *22* (12), 2929−38.
(32) Tummers, Q. R.; Hoogstins, C. E.; Gaarenstroom, K. N.; de Kroon, C. D.; van Poelgeest, M. I.; Vuyk, J.; Bosse, T.; Smit, V. T.; van de Velde, C. J.; Cohen, A. F.; Low, P. S.; Burggraaf, J.; Vahrmeijer, A. L. Intraoperative imaging of folate receptor alpha positive ovarian and breast cancer using the tumor specific agent EC17. *Oncotarget* **2016**, *7* (22), 32144−55.
(33) De Jesus, E.; Keating, J. J.; Kularatne, S. A.; Jiang, J.; Judy, R.; Predina, J.; Nie, S.; Low, P.; Singhal, S. Comparison of Folate Receptor Targeted Optical Contrast Agents for Intraoperative Molecular Imaging. *Int. J. Mol. Imaging* **2015**, *2015*, 469047.
(34) Ledermann, J. A.; Canevari, S.; Thigpen, T. Targeting the folate receptor: diagnostic and therapeutic approaches to personalize cancer treatments. *Annals of oncology: official journal of the European Society for Medical Oncology* **2015**, *26* (10), 2034−43.
(35) Koch, M.; de Jong, J. S.; Glatz, J.; Symvoulidis, P.; Lamberts, L. E.; Adams, A. L.; Kranendonk, M. E.; Terwisscha van Scheltinga, A. G.; Aichler, M.; Jansen, L.; de Vries, J.; Lub-de Hooge, M. N.; Schroder, C. P.; Jorritsma-Smit, A.; Linssen, M. D.; de Boer, E.; van der Vegt, B.; Nagengast, W. B.; Elias, S. G.; Oliveira, S.; Witkamp, A. J.; Mali, W. P.; Van der Wall, E.; Garcia-Allende, P. B.; van Diest, P. J.; de Vries, E. G.; Walch, A.; van Dam, G. M.; Ntziachristos, V. Threshold Analysis and Biodistribution of Fluorescently Labeled Bevacizumab in Human Breast Cancer. *Cancer Res.* **2017**, *77*, 623.
(36) Hernandez, R.; Heskamp, S.; Rijpkema, M.; Bos, D. L.; Goldenberg, D. M.; McBride, W. J.; Morgenstern, A.; Bruchertseifer, F.; Cai, W.; Boerman, O. C. Preventing Radiobleaching of Cyanine Fluorophores Enhances Stability of Nuclear/NIRF Multimodality Imaging Agents. *Theranostics* **2017**, *7* (1), 1−8.

DOI: 10.1021/acs.molpharmaceut.7b00464
Mol. Pharmaceutics 2017, 14, 3457−3463